nature nanotechnology

SUPPLEMENTARY INFORMATION

https://doi.org/10.1038/s41565-019-0548-1

In the format provided by the authors and unedited.

Hot-electron dynamics in quantum dots manipulated by spin-exchange Auger interactions

Rohan Singh[1], Wenyong Liu[1], Jaehoon Lim[1,2,3], István Robel[1] and Victor I. Klimov[1]*

[1]Chemistry Division, Los Alamos National Laboratory, Los Alamos, NM, USA. [2]Department of Chemical Engineering, Ajou University, Suwon, Republic of Korea. [3]Department of Energy System Research, Ajou University, Suwon, Republic of Korea. *e-mail: klimov@lanl.gov

Supplementary Note 1. Modeling of carrier dynamics in the case of low-intensity, near-band-edge excitation

Here we use a simplified 'excitonic' description of excitation exchange between intrinsic-QD and Mn-ion states (Fig. 1e and Supplementary Fig. 8a). We quantify populations of these states in terms of average per-dot occupancies: n_X (band-edge exciton) and n_{Mn} (excited Mn state). Since for conditions of our experiments, the rates of both direct and back energy transfer (DET and BET, respectively) in a QD-Mn system are much faster than any recombination rates, we neglect population losses on the DET and BET time scales, which implies that $n_X + n_{Mn} = n_0 = const$, where n_0 is the total number of originally injected excitations at time zero ($t = 0$).

When $n_0 < 1$ (low-pump-level regime), the evolution of n_X and n_{Mn} can be described by the following rate equations:

$$\dot{n}_X = -k_D\, n_X + k_B\, n_{Mn}, \qquad (1)$$

$$\dot{n}_{Mn} = k_D\, n_X - k_B\, n_{Mn}, \qquad (2)$$

where k_D and k_B are the DET and BET rates, respectively. They are related to corresponding time constants by $\tau_D = 1/k_D$ and $\tau_B = 1/k_B$. The system of eqs 1 and 2 has an analytical solution. In particular, in the case when at $t = 0$, $n_X = n_0$ and $n_{Mn} = 0$, the occupancy of the QD 1S excitonic level evolves as follows:

$$n_x(t) = n_0 \frac{1}{1+f}\left[1 + f e^{-k_{1S}t}\right], \qquad (3)$$

where $k_{1S} = k_D + k_B = k_D(1 + f^{-1})$ and $f = k_D/k_B$. This analytical solution is used in the analysis of 1S bleach dynamics recorded in a transient absorption (TA) experiment with near-band-edge excitation (Fig. 2a of the main text).

In our analysis, we account for the existence of two QD sub-ensembles, one with internally located dopants and the other, with surface dopants. These two sub-ensembles are characterized by 'fast' ($k_{D,i}$ and $k_{B,i}$; "i" stands for "internal") and 'slow' ($k_{D,s}$ and $k_{B,s}$, "s" stands for "surface") transfer rates (left and right panels of Supplementary Fig. 8a, respectively). Further, in our analysis, we compare experimentally measured traces to modeling after theoretical traces are convolved with an instrument response function (IRF) approximated by a Gaussian with a 110-fs half-width at half maximum.

Supplementary Note 2. Modeling of carrier dynamics in the case of low-intensity, hot-carrier excitation

To model carrier dynamics in the case of above band-edge excitation at 3.61 eV, we modify eqs 1 and 2 by adding a rate equation for the occupancy of the excited (hot) exciton (n_{X^*}) and introducing a characteristic carrier cooling rate k_c connected to a characteristic cooling time (τ_c) by $\tau_c = 1/ k_c$ (Supplementary Fig. 8b). The updated system of rate equations is presented as follows:

$$\dot{n}_{X^*} = -(k_c + k_D)\, n_{X^*} \qquad (4)$$

$$\dot{n}_X = k_c\, n_{X^*} - k_D\, n_X + k_B\, n_{Mn} \qquad (5)$$

$$\dot{n}_{Mn} = k_D\, (n_{X^*} + n_X) - k_B\, n_{Mn} \qquad (6)$$

To solve these equations, we use the following set of initial conditions: $n_{X^*}(0) = n_0$ and $n_X(0\ \text{ps}) = n_{Mn}(0\ \text{ps}) = 0$. This yields the following solution for n_X:

$$n_X(t) = n_0 \frac{1}{1+f}\left[1 + f e^{-\left(1+\frac{1}{f}\right)k_D t} - (1+f)e^{-(1+g)k_D t}\right], \quad (7)$$

where $g = k_c/k_D$. The examples of temporal behaviors of n_X predicted by eq 7 are displayed in Supplementary Fig. 5a. These examples corresponds to experimentally measured DET times for internal ($\tau_{D,i}$ = 140 fs, red line) and surface ($\tau_{D,s}$ = 2.6 ps; blue line) dopants and the cooling time τ_c = 500 fs. The black line shows the superposition of these traces assuming that the ratio between the fractions of internally (p_i) and surface (p_s) doped dots is one. These results reproduce the experimentally observed delay (t_m) of the peak band-edge signal, as well as the reduction in its amplitude ($n_{X,m}$); see Fig. 2a (blue squares). As illustrated in Supplementary Fig. 5b, $n_{X,m}$ depends on the ratio of the cooling and DET rates (g) and decreases from ~0.7 to ~0.3 as g decreases from 10 to 1.

Supplementary Note 3. Modeling of carrier dynamics in the case of high-intensity, hot-carrier excitation

To model the regime of high excitation intensities when multiple hot excitons are injected in a dot, we modify the rate equations introduced in the previous section by including a spin-exchange Auger term, which is proportional to $k_{A,i}n_{X^*}\, n_{Mn}$ ($k_{A,i}$ is the Auger interaction rate in QDs with the internal dopant). This term is responsible for transfer of a hot electron from state X* to a 'vacuum' level outside the dot (Fig. 3c and Supplementary Fig. 8c, left panel). We denote the occupancy of the 'vacuum' state as n_V and its recombination rate as k_V. We further account for spin-exchange interactions of a band-edge exciton (X) with an excited Mn ion introducing the term proportional to $k_{A,i}n_X\, n_{Mn}$. This process promotes the band-edge exciton to the X* state without leading to QD ionization (Supplementary Fig. 8c, right panel). In addition, we account for the fact that the band-edge level can only accommodate 2 excitons. We also limit

the maximum number of per-dot Mn-based excitations by N_{Mn} and the number of available 'vacuum' states by N_V. The resulting rate equations are:

$$\dot{n}_{X^*} = -k_c\, n_{X^*}\left(1-\frac{n_X}{2}\right) - k_D\, n_{X^*}\,(N_{Mn}-n_{Mn}) - k_{ion}\, n_{X^*}\, n_{Mn}\,(N_V-n_V) + k_{A,i}\, n_X\, n_{Mn}, \quad (8)$$

$$\dot{n}_X = k_c\, n_{X^*}\left(1-\frac{n_X}{2}\right) - k_D n_X\,(N_{Mn}-n_{Mn}) + k_B\, n_{Mn}\left(1-\frac{n_X}{2}\right) - k_{A,i}\, n_X n_{Mn}, \quad (9)$$

$$\dot{n}_{Mn} = k_D(n_{X^*}+n_X)(N_{Mn}-n_{Mn}) - k_B n_{Mn}\left(1-\frac{n_X}{2}\right) - k_{A,I} n_{X^*} n_{Mn}(N_V-n_V) - k_{A,I} n_X n_{Mn}\,, \quad (10)$$

$$\dot{n}_V = k_{A,i}\, n_{X^*}\, n_{Mn}\,(N_V-n_V) - k_V n_V\,. \quad (11)$$

Since Auger ionization is only observed for the case of hot-carrier excitation, it occurs in QDs with internal dopants wherein spin-exchange interactions are sufficiently fast to favorably compete with intra-band cooling. Therefore, in our modeling we use $k_D = k_{D,i} = 1/140$ fs^{-1}. Given that most of the internally doped dots contains only one Mn ion, we use $N_{Mn} = 1$. Further, we assume that $N_V = 1$, which can be justified by the fact that an electric field generated following ejection of the first electron creates a potential barrier, which prevents the second ionization event in the same dot. After making these assumptions, we numerically solve eqs 8 – 11 as a function of per-dot number of initially injected hot excitons (n_0). Then, we compare the calculated dependence of n_V *versus* n_0 with the measured dependence of the amplitude of a Stark-effect related photoinduced absorption feature on pump fluence. As can be seen from Fig. 3d of the main text, this model (lines) allows for accurate description of experimental observations (symbols). Based on the modeling, $k_{A,i} = 1/150$ fs^{-1}.

We would like to point out that while this model captures essential features of the conducted experiments, it provides only an approximate description of carrier dynamics in a coupled QD-Mn-ion system. A more accurate description would require consideration of a much greater

number of coupled rate equations in order to separately treat QDs with different numbers of excitons and account for the explicit configuration of each excited state. Because of its simplified character, this model is not well suited for treating the case of low-intensity excitation, which corresponds to injection of a single exciton per dot. While it will allow one to reproduce general trends observed in the limit of $\langle N_{ph} \rangle < 1$, the models introduced in the previous sections (1 and 2) provide a more accurate description of the regime of low excitation fluences.

a

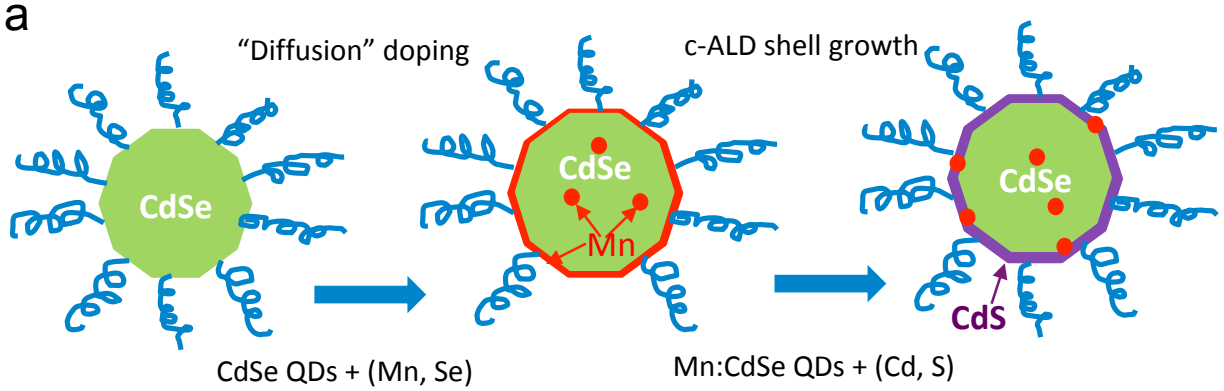

b

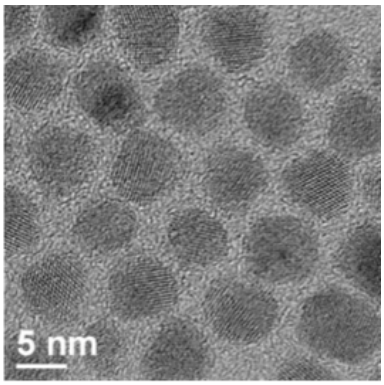

c

	Elemental ratio Cd:Se:Mn	Core diameter (nm)	Number of anions (Se)	Nominal number of Mn ions per QD
Mn:CdSe QDs	1.2:1.0:0.12	3.1	278	33

Supplementary Figure 1| a, Schematic illustration of synthesis of Mn:CdSe(core)/CdS(shell) QDs. It starts with the preparation of wurtzite CdSe cores (left) that are then reacted with Mn precursors. Mn is first incorporated in the surface layer and then some of the surface dopants diffuse into the core interior (middle). Finally, the doped CdSe cores are overcoated with CdS (right) using colloidal atomic layer deposition (c-ALD). This procedure results in partial removal of surface dopants. **b,** An example of a transmission electron microscopy image of Mn:CdSe/CdS QDs with the 4.6-nm core size and ~1-nm thick shell. **c,** Elemental analysis of as-prepared 3.1-nm CdSe cores. It indicates that the approximate number of Mn ions per dot is 33. According to elemental mapping using energy-dispersive X-ray spectroscopy, most of the dopants resided on the core surface. Some of them are replaced with Cd during deposition of the CdS shell.

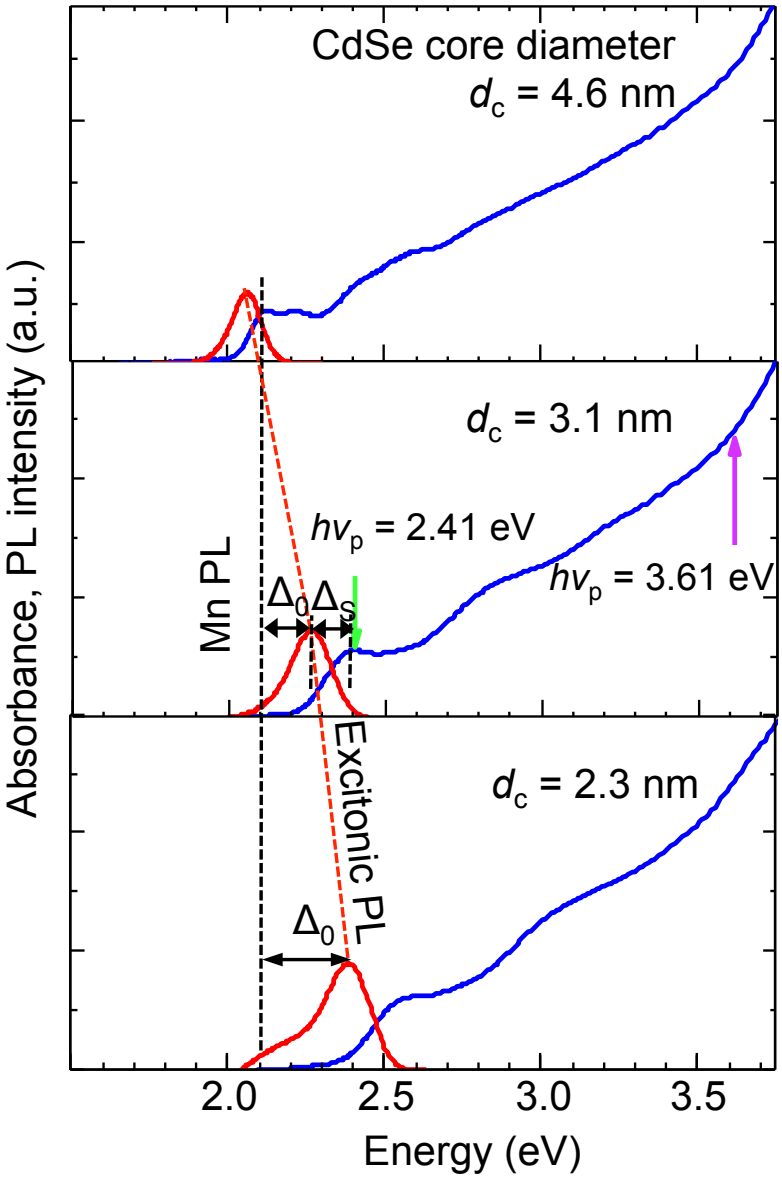

Supplementary Figure 2| Absorption (blue) and emission (red) spectra of Mn:CdSe/CdS QDs with mean core diameters d_c = 4.6 nm (top), 3.1 nm (middle), and 2.3 nm (bottom). The black dashed line marks the position of the Mn *d-d* transition. The red dashed lines track the position of the emission peak due to the intrinsic band-edge QD transition. Δ_0 is the energetic driving force for the QD-to-Mn energy transfer. Δ_S is the Stokes shift. The green and magenta arrows show the pump-photon energies used in transient absorption measurements.

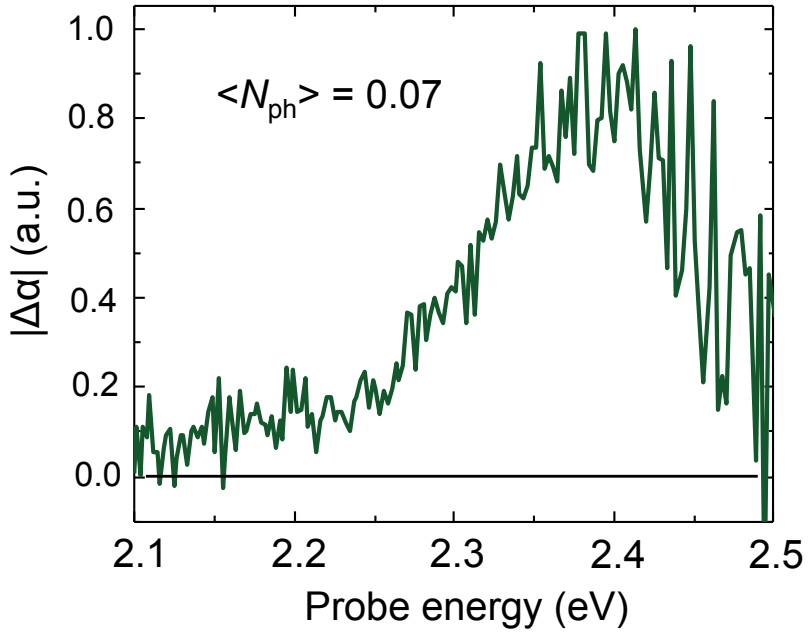

Supplementary Figure 3| Early time transient absorption (TA) spectrum of Mn-doped QDs with the core diameter d_c = 3.1 nm recorded for pump-probe delay Δt = 3 ps. The pump photon energy is $h\nu_p$ = 2.41 eV, and the pump fluence evaluated in terms of the average number of photons absorbed per dot, per pulse is $\langle N_{ph} \rangle$ = 0.07.

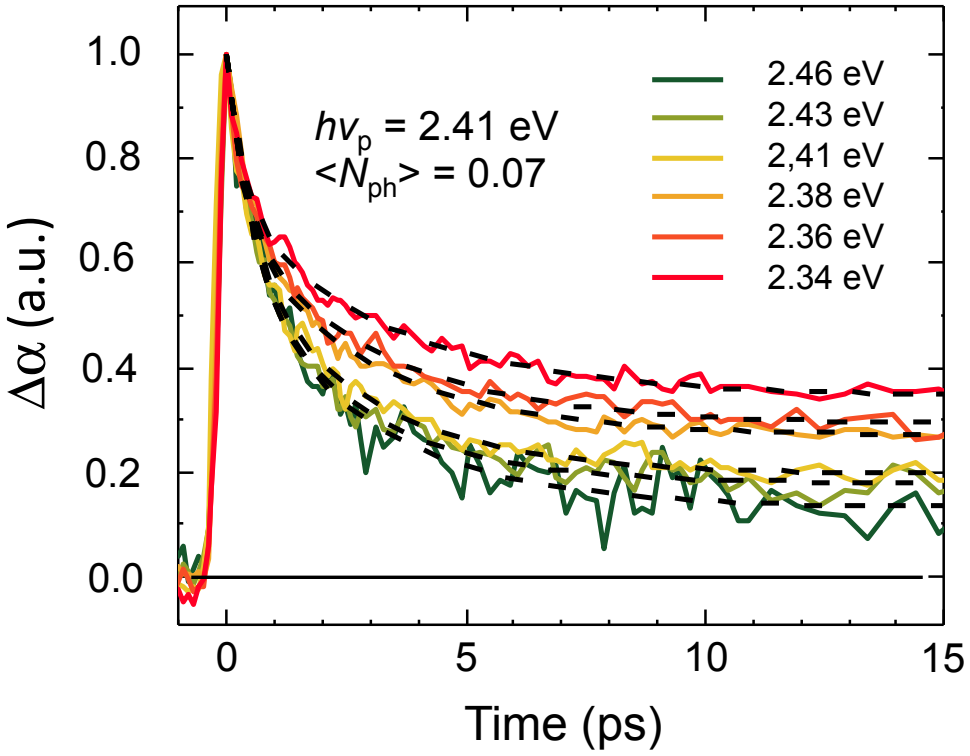

Supplementary Figure 4| 1S bleach dynamics for Mn-doped CdSe/CdS QDs with 3.1-nm CdSe cores recorded using band-edge excitation ($h\nu_p$ = 2.41 eV) and different probe energies indicated in the legend (coloured lines). The black dashed lines are the results of the modeling using formalism described in Supplementary Note 1. The calculated traces are convolved with the experimental IRF. These data were used to obtain the dependence of the ratio of the rate of direct energy transfer (DET, k_D) and that of back energy transfer (BET, k_B) on probe energy (see Fig. 2c in the main text).

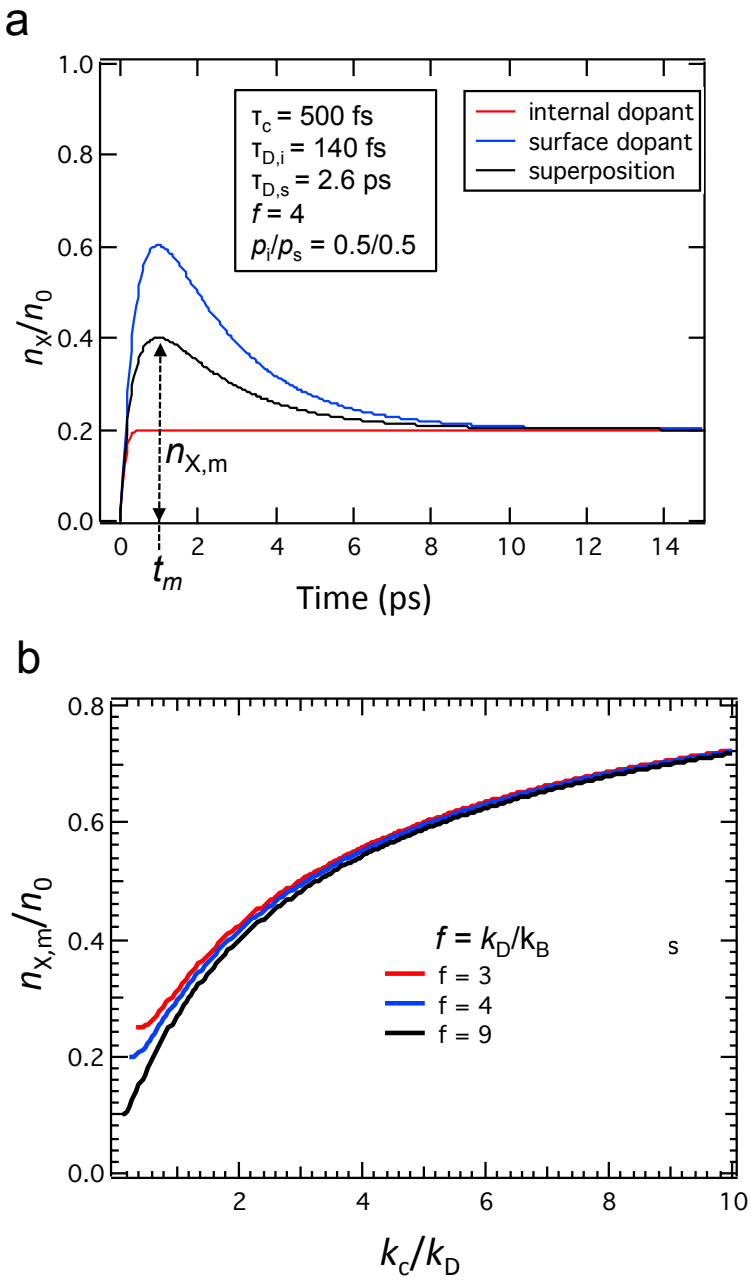

Supplementary Figure 5| a, Modeling of occupancy of the band-edge QD exciton state (n_X) in the case of high-photon energy excitation ($h\nu_p$ = 3.61 eV), which corresponds to injection of a single hot exciton per dot (Supplementary Note 2). The traces have been obtained using the same cooling time (τ_c = 500 fs) and two different DET times that correspond to internal ($\tau_{D,i}$ = 140 fs, red) and surface ($\tau_{D,s}$ = 2.6 ps, blue) dopants. The black trace is a superposition of the two assuming equal fractions of dots with internal (p_i) and surface (p_s) dopants. **b,** The dependence of the peak occupancy of the band-edge state on the ratio of the cooling rate ($k_c = 1/\tau_c$) and the DET rate for several ratios of the DET and BET rates (indicated in the legend).

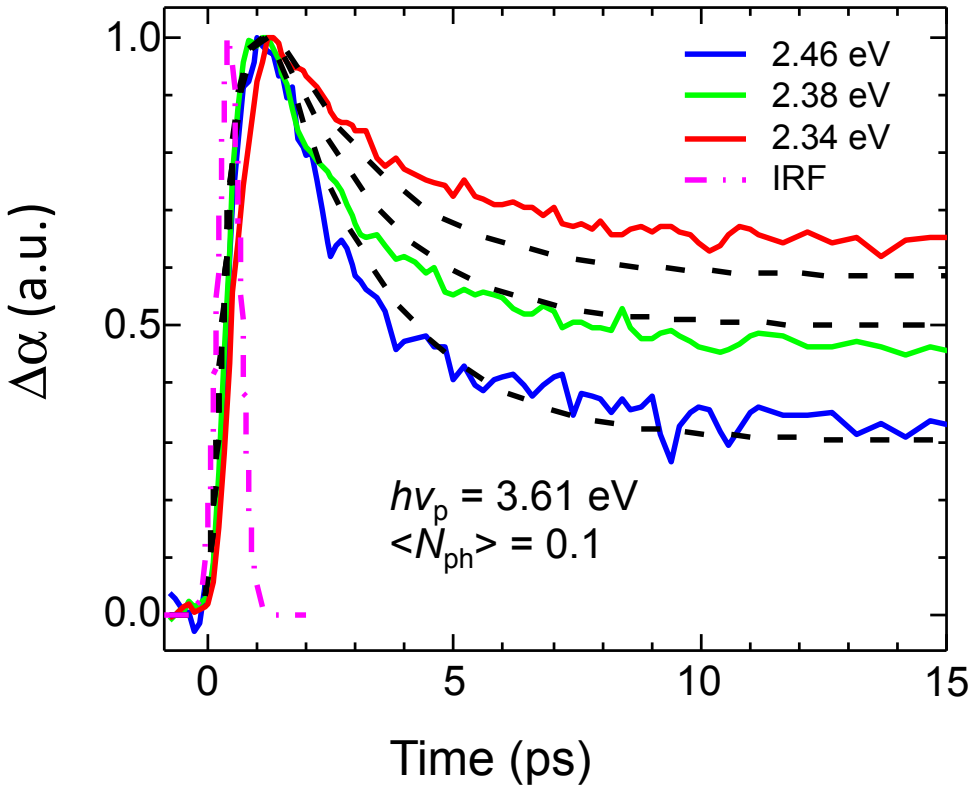

Supplementary Figure 6| a, 1S bleach dynamics for Mn-doped CdSe/CdS QDs with 3.1-nm CdSe cores recorded using high-photon-energy excitation ($h\nu_p$ = 3.61 eV) and different probe energies indicated in the legend (coloured solid lines). The black dashed lines are modeling using the formalism described in Supplementary Note 2. The calculated traces are convolved with the experimental IRF (magenta dashed-dotted line).

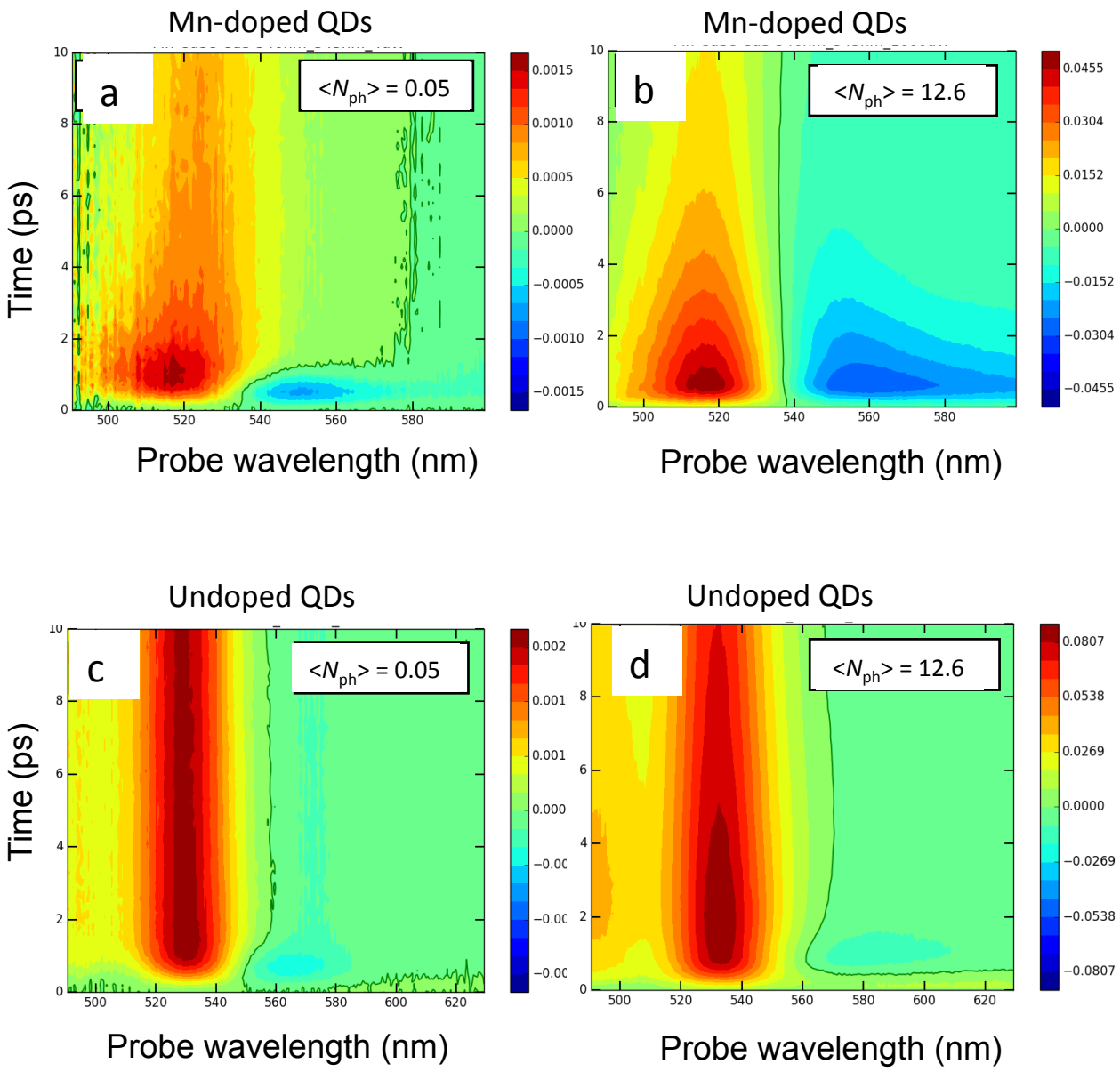

Supplementary Figure 7| Two-dimensional TA maps that show the amplitude of the TA signal (colour-scale representation) as a function of probe wavelength (horizontal axis) and pump-probe delay time (vertical axis) for Mn-doped QDs with 3.1-nm CdSe cores (**a,b**) in comparison to TA data for the reference undoped sample (**c,d**). These data are collected using high-photon energy excitation with $h\nu_p$ = 3.61 eV and low (**a,c**) and high (**b,d**) pump fluences that correspond, respectively, to $\langle N_p \rangle$ = 0.05 and 12.6. A strong photoinduced absorption feature at ~560 nm, which develops in the doped sample at high pump fluence (**b**), is a signature of QD ionization. It is absent in the undoped sample (**d**).

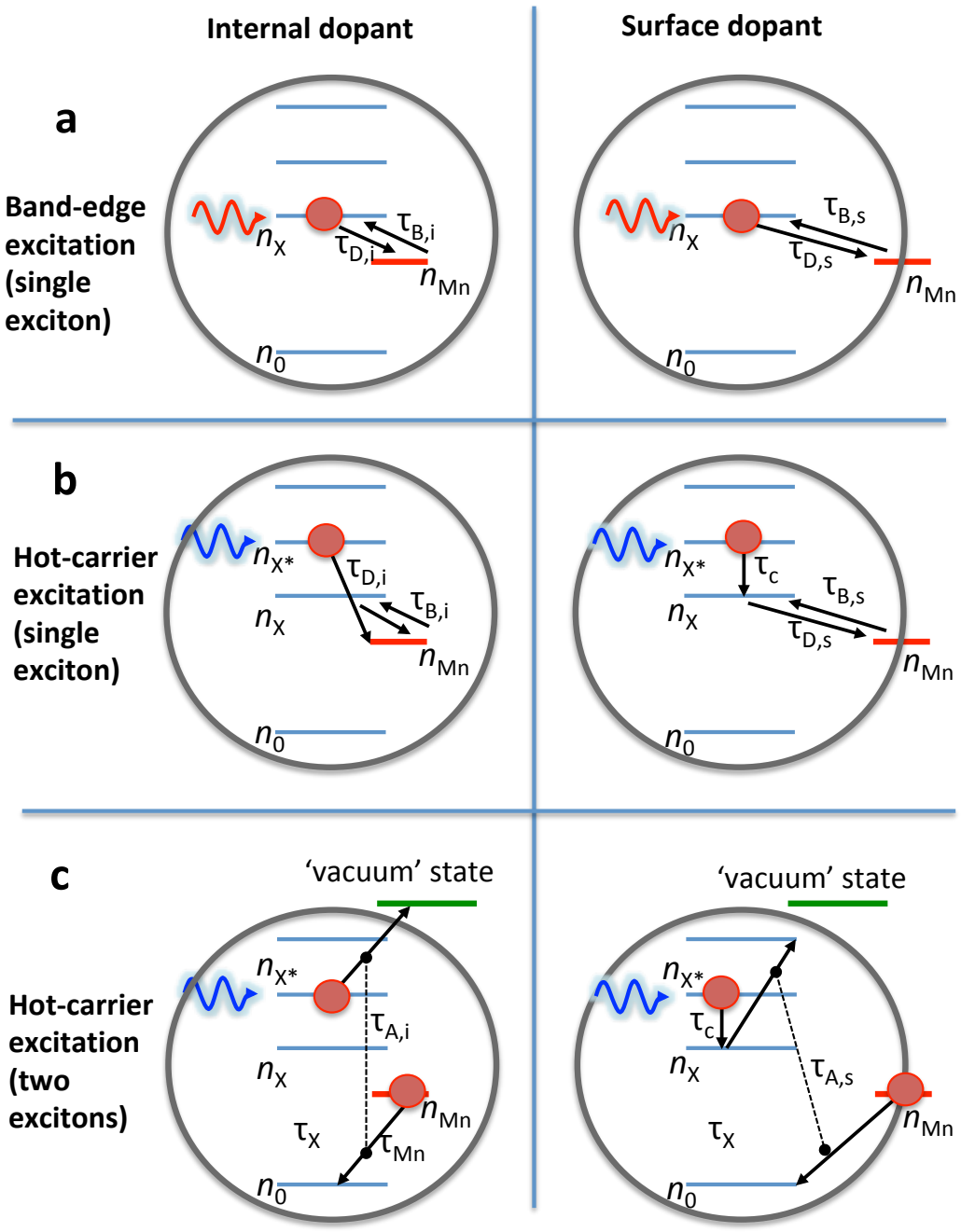

Supplementary Figure 8| 'Excitonic' representation of various energy-exchange regimes between the intrinsic QD states and internal (left) and surface (right) dopants for the cases of weak (single-exciton) band-edge excitation (a), weak (single-exciton) high-spectral-energy excitation (b), and strong (two-exciton) high-spectral-energy excitation (c). The per-dot occupancies of the ground, band-edge-exciton, Mn-dopant, and 'hot'-exciton states are denoted as n_0, n_X, n_{Mn}, and n_{X*}, respectively.